Influence of chitosan on the mechanical and biological properties of HDPE for biomedical applications

Polymer Testing 91 (2020) 106610

Contents lists available at ScienceDirect

Polymer Testing

journal homepage: http://www.elsevier.com/locate/polytest

Material Properties

Influence of chitosan on the mechanical and biological properties of HDPE for biomedical applications

M. Di Maro [a,b], M.G. Faga [a,*], G. Malucelli [c], F.D. Mussano [d], T. Genova [d], R.E. Morsi [e,f], A. Hamdy [e], D. Duraccio [a]

[a] Istituto per le Macchine Agricole e Movimento Terra (IMAMOTER)-UOS di Torino, Consiglio Nazionale delle Ricerche, Strada delle Cacce 73, 10135, Torino, Italy
[b] Dipartimento di Scienze Chimiche,della Vita e della Sostenibilità, Università degli Studi di Parma, Parco Area delle Scienze, 11/A, 43124, Parma PR, Italy
[c] Politecnico di Torino - Dipartimento di Scienza Applicata e Tecnologia, Viale Teresa Michel 5, 15121, Alessandria, Italy
[d] Dipartimento di Scienze Chirurgiche CIR Dental School, Università di Torino, via Nizza 230, 10126, Torino, Italy
[e] Egyptian Petroleum Research Institute, 11727, Cairo, Egypt
[f] Istituto per la Sintesi Organica e la Fotoreattività (ISOF), Consiglio Nazionale delle Ricerche, Via P. Gobetti, 101 - 40129, Bologna, Italy

A B S T R A C T

High density polyethylene (HDPE) is widely used in biomedical field, except when strong cell-material interactions and high mechanical properties are required. To address this pitfall, two kinds of chitosan in different amounts were used as filler in the present research. Composites were prepared by melt extrusion process and their microstructural, thermal and mechanical properties were widely investigated. Also roughness and wettability were studied, as features of paramount importance in dictating cell response.

Both types of chitosan endowed HDPE with higher Young modulus and lower elongation at break. Interestingly, fibroblast adhesion and viability were enhanced when a low amount of filler was used. The interaction of HDPE/chitosan composites with biological environment was investigated for the first time in order to assess the feasibility of these composites as materials for biomedical application.

1. Introduction

Polyethylene (PE), polycaprolactone (PCL), polyglycolic acid (PGA), polylactic acid (PLA) and polyether ether ketone (PEEK) are promising synthetic polymers for tissue engineering applications due to their biocompatibility and mechanical properties [1]. High density polyethylene (HDPE) is a highly versatile biomaterial already used in pre-clinical studies and clinical practice with interesting outcomes [2]. Among the hallmarks prompting the diffusion of PE, there are low cost, ease of processing, and high ductility, which allows the incorporation of a large variety of particles in the polymer [3]. Thus, novel composites, even charged with a high amount of fillers, can be processed with the most common and cheapest melt extrusion techniques [3,4]. HDPE was initially synthesized with a porous surface conveniently allowing rapid tissue in-growth, to overcome its bio-inertia. However, high porosity significantly decreases the mechanical properties of the biomaterial and can cause its premature failure [5–7]. Hence, alternative methods for increasing cells interaction were required. Although a number of porous HDPE bone scaffolds had been patented [8,9] and commercialized for cranial reconstruction, several studies aimed at increasing biological integration and possibly longevity of the biomaterial recurring to a variety of fillers. Such is the case of hydroxyapatite, known indeed since the early '80s [10–14], and, more recently, bioglasses [15,16], which were added to HDPE to enhance bioactivity.

As a promising filler capable to ameliorate, also mechanically, PE, some authors proposed chitosan, describing positive features in terms of thermal, rheological, mechanical and morphological behavior [17–19]. This is consistent with the remarkable interest chitosan elicits as it is made from an abundant renewable source and it is compatible, effective and versatile [20,21]. Indeed, chitosan is obtained by deacetylation of chitin, a polysaccharide widely distributed in nature in the exoskeleton of crustaceans, in certain fungi and insects [22,23]. Chitosan has an excellent biocompatibility, low toxicity, antimicrobial activity and low immunogenicity that provide a wide range of opportunities for further development [24–27]. Chitosan alone or mixed with polymers has been widely studied for different biological applications, including wound healing, drug delivery, gene therapy, bioimaging applications and tissue engineering [27,28]. Due to its poor mechanical properties however, chitosan cannot be considered *per se* as tissue analogue replacement [17].

* Corresponding author.
E-mail address: m.faga@imamoter.cnr.it (M.G. Faga).

https://doi.org/10.1016/j.polymertesting.2020.106610
Received 6 March 2020; Received in revised form 1 May 2020; Accepted 9 May 2020
Available online 16 May 2020

Table 1
Properties of chitosan powders.

	DD (%)[a]	T_g (°C)[b]	$\chi_{C\ (\%)}$[c]	χ_{CI} (%)[c]
CM chitosan	87.0	157	41.0	69.9
CN chitosan	97.0	150	21.0	38.7

[a] measured by FTIR.
[b] measured by DSC.
[c] measured by WAXD.

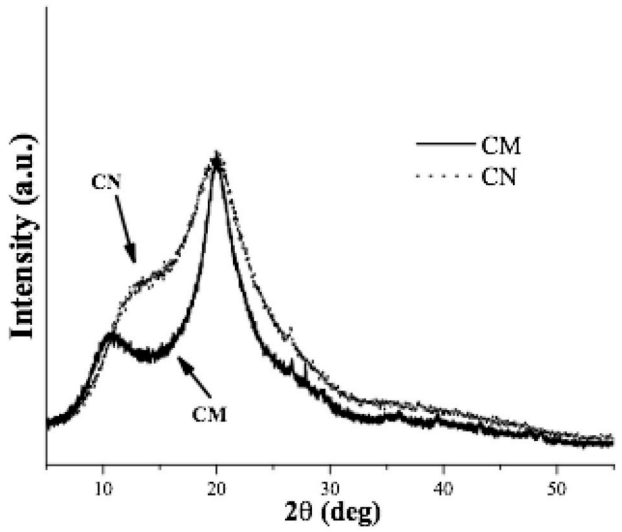

Fig. 1. WAXD patterns of CM and CN.

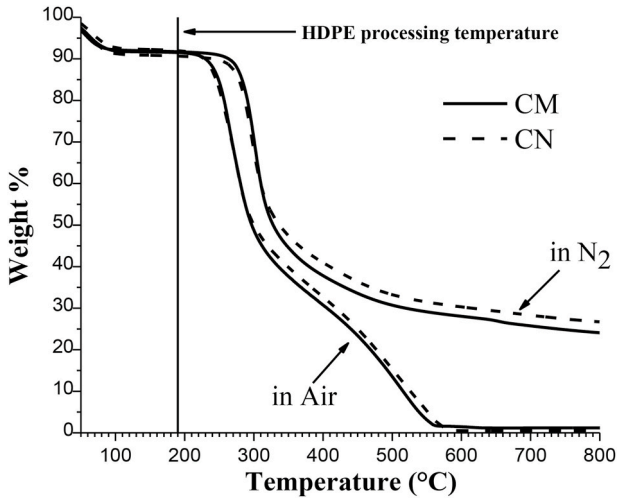

Fig. 2. TG curves of chitosan M and N, performed in N_2 and in air at 10 °C/min.

For all the above reasons, the use of chitosan as filler in HDPE-based composites has been considered in this work as regards the preparation of subdermal cranio-facial scaffolds. Large defects especially affecting ears and nose that have been rehabilitated so far mainly by maxillofacial prostheses are on the verge of benefiting from advanced surgical techniques and tissue regeneration protocols [29].

It is the authors' belief that, under this perspective, the interaction of HDPE/chitosan composites with biological environment is unprecedented. Indeed, although previous papers were dedicated to HDPE/chitosan [12,17,18] and LDPE/chitosan [19,30], they were mainly focused on the compatibilization of the components and on the food packaging applications. Here, two kinds of chitosan based composites have been prepared by melt mixing and characterized to obtain a material with both satisfactory mechanical properties and cells interaction. As starting materials, two kind of chitosan endowed with a different amount of residual acetyl groups were selected.

2. Materials and methods

2.1. Materials and composites preparation

High Density Polyethylene (HDPE, melt flow index: 0.4g/10min at 190 °C/2.16 kg) resin grade was kindly supplied by Lyondell – Basel. Two chitosan grades were purchased by G.T.C. Bio Corporation: high viscosity chitosan (2000 cps) with deacetylation degree >80% (herein after coded as CM) and medium-low viscosity chitosan (140 cps) with deacetylation degree of 96.1%.

Before using, chitosan was dried in a vacuum oven at 60 °C for 12 h to remove water. HDPE/chitosan composites were prepared by using a DSM xplore Micro 15cc twin-screw compounder working at 190 °C (processing time: 5 min). The extruded materials were compressed with a Collin P200T press at 210 °C for 2 min to obtain 0.5 mm thick sheets. Three mixing ratios of HDPE/chitosan (wt/wt) for each type of chitosan were prepared: 99/1, 98/2 and 95/5.

2.2. Characterization

Fourier Transform IR (FTIR) experiments were performed on CM and CN by using a PerkinElmer Frontier FT-IR instrument, in order to verify the deacetylation degree (DD) of both materials. Spectra were recorded as an average of 200 scans in the range 4000–400 cm^{-1} with a spectral resolution of 4 cm^{-1}. Pellets were prepared by mixing 2 mg of chitosan powder, previously dried at 60°C under reduced pressure for 6 h, with 100 mg KBr, previously dried over night at 80 °C. According to the method proposed by Baxter et al. [31], deacetylation degree (DD) was evaluated using the amide-I band ($\nu = 1655\ cm^{-1}$) as the analytical band and the hydroxyl band ($\nu = 3450\ cm^{-1}$) as the internal reference band. DD was calculated by the following equation:

$$DD\ (\%) = 100 - [(A_{1655}/A_{3450}) \times 115] \quad (1)$$

Scanning Electron Microscopy (Zeiss Evo 50 XVP with LaB6 source) was employed for investigating the morphology, dispersion and distribution of CM and CN particles within the polymer matrix. SEM analysis was performed on the cross section cryogenically fractured in liquid nitrogen. All the samples were coated with a thin layer of gold (few nanometers) and then analysed.

X-rays diffraction patterns (WAXD) of the chitosan particles and their composites with HDPE were obtained by using a PW3040/60 X'Pert PRO MPD diffractometer from PANalytical working at 45 kV and 40 mA, and using the Bragg–Brentano geometry. The source is a high-power ceramic tube PW3373/10 LFF with Cu anode. WAXD profiles were acquired using a Ni-filtered Cu-Kα radiation (λ = 0.15418 nm) with a continuous scan of 0.04°/s in the range 5–70°. The crystallinity index (χ_{cA}) of CM and CN was calculated as the ratio between the area of the crystalline phase, determined after correction of the baseline for amorphous regions, and the total area of the XRD pattern, computed after the general baseline correction. Another technique for evaluating the crystallinity index of chitosan was also used for comparison: according to Focher's method [32], χ_{cI} is calculated by the ratio between the maximum intensity, I_{110}, at 2θ = 20° of the (110) lattice diffraction and that of the amorphous diffraction, I_{am}, at 2θ = 16°, using equation (2).

$$\chi_{cI} = (I_{110} - I_{am})/\ I_{110} \quad (2)$$

In order to study the influence of chitosan on the crystallinity of HDPE, the crystallinity index was measured by the ratio between the intensity of diffraction peaks belonging to the crystalline phase and the intensity of the total sample diffraction pattern. The intensity of the

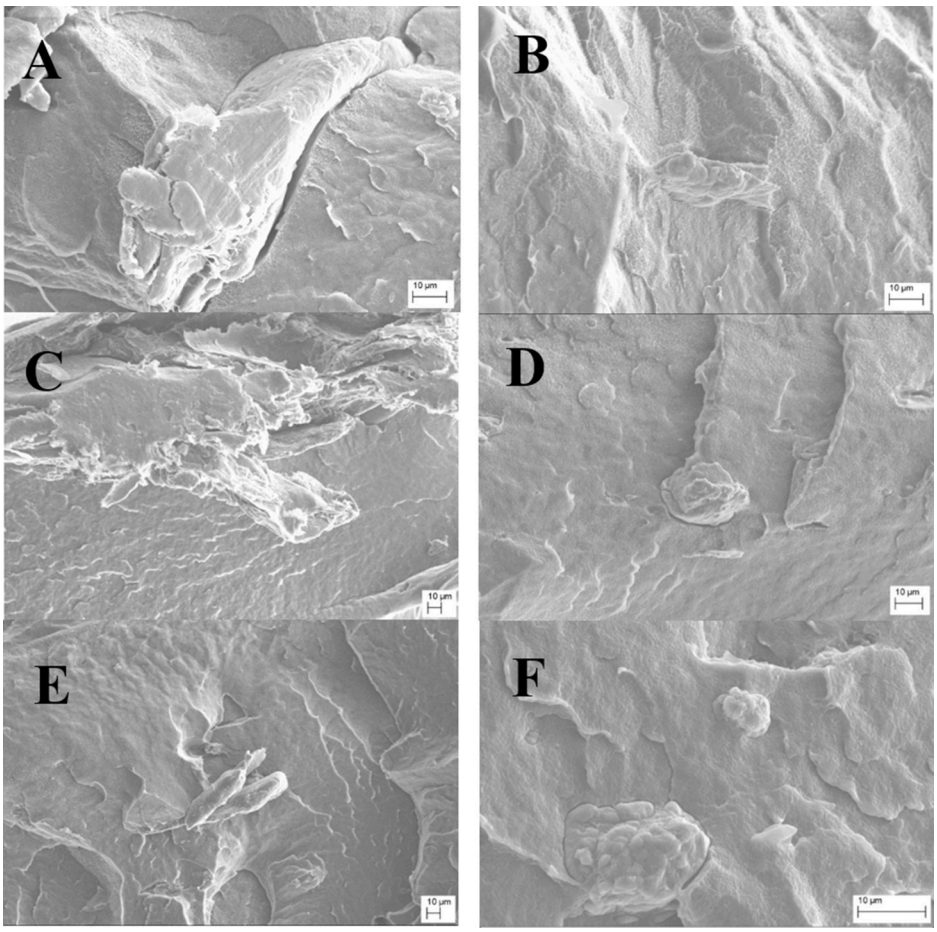

Fig. 3. SEM micrographs of A) HDPE/CM 99/1, B) HDPE/CN 99/1, C) HDPE/CM 98/2, D) HDPE/CN 98/2, E) HDPE/CM 95/5, F) HDPE/CN 95/5.

crystalline phase was determined by subtracting the amorphous phase from the total intensity of the diffraction spectra. The profile of amorphous phase was approximated using the average spectrum of the profiles of HDPE melt at 180, 190 and 200 °C.

The equation used to quantify the crystallinity degree of HDPE is:

$$x_A = \frac{\left[\frac{I_{TOT} - Iam}{I_{TOT}}\right]}{y\ PE} * 100 \quad (3)$$

where *y PE* is the mass fraction of HDPE in the composites and it is 1 for the neat polymer and 0.95 for the HDPE/chitosan 95/5.

Glass transition temperatures of CM and CN were measured by Differential Scanning Calorimetry (DSC), using a TA DSC Q20 (USA) with a heating rate of 20 °C/min. The experiments were carried out using 3.0 ± 0.5 mg of material, according to the following cycle: (1) heating up from 25°C to 190°C at 20 °C/min; (2) cooling down to 25 °C at 20 °C/min; (3) heating up from 25 °C to 190 °C at 20 °C/min.

Thermogravimetric analysis (TGA) was performed in nitrogen and in air from 50°C to 800 °C with a heating rate of 10 °C/min, using a TA Discovery thermo balance (TA Instruments) (experimental error: ± 0.5% wt., ±1 °C). The samples (ca. 10 mg) were placed in open platinum pans and fluxed with nitrogen (gas flow: 25 ml/min).

The tensile properties of HDPE/chitosan composites were measured using an Instron 5966 tensile tester. The experiments were conductd on compression-molded plates, according to the standard test method ASTM D882 at room temperature. The specimens were approximately 0.5 mm thick and 5 mm wide. The parameters at break (elongation (ε_b) and strain (σ_b)) were determined with constant deformation rate, in order to maintain the ratio v/L_0 equal to 10 mm/(mm* min) (where v = deformation rate and L_0 = initial length of the specimen). The Young modulus E was also measured with the ratio v/L_0 equal to 0.1 mm/(mm*min). The mean values of the mechanical properties were averaged over at least five independent tests.

Dynamic-mechanical (DMTA) analyses were performed using a Triton TTDMA (TA Instruments) in dual cantilever bending configuration. The following experimental conditions were adopted: temperature range from −150°C to 80 °C, heating rate of 3°C/min, 1 Hz of frequency. Storage modulus (E'), loss modulus (E") and tanδ curve were recorded. For each formulation, the tests were repeated at least three times and the experimental error was calculated as standard deviation for all the measured parameters.

Wettability based on Sessile Droplet Contact Angle Measurement was evaluated with a Kruss DSA 100 apparatus, provided with a 25x optical zoom. The analysis was performed with double distilled water at room temperature. Contact angles were measured on at least five independent positions on the sample surface.

A contact profilometer (Form Talysurf 120) equipped with a 2 µm diamond conical stylus was used for evaluating the surface roughness. The arithmetic mean deviation of the assessed profile, Ra, was measured by considering a sampling length of 0.8 mm and a cut-off of 0.8. The data concerning the surface roughness were not normally distributed (Kolmogorov-Smirnovtest, Z = 0.100, p = 0.007), therefore a non-parametrical analysis with the Kruskal-Wallis test was used. Pairwise comparisons were carried out using Wilcoxon rank sum test with a significance level of $p = 0.05$.

In order to evaluate the biological effects of chitosan in the HDPE composites, fibroblastic cell line NHDF (ECACC, Salisbury, UK) were used in vitro assay. Cells were maintained in DMEM (Dulbecco's

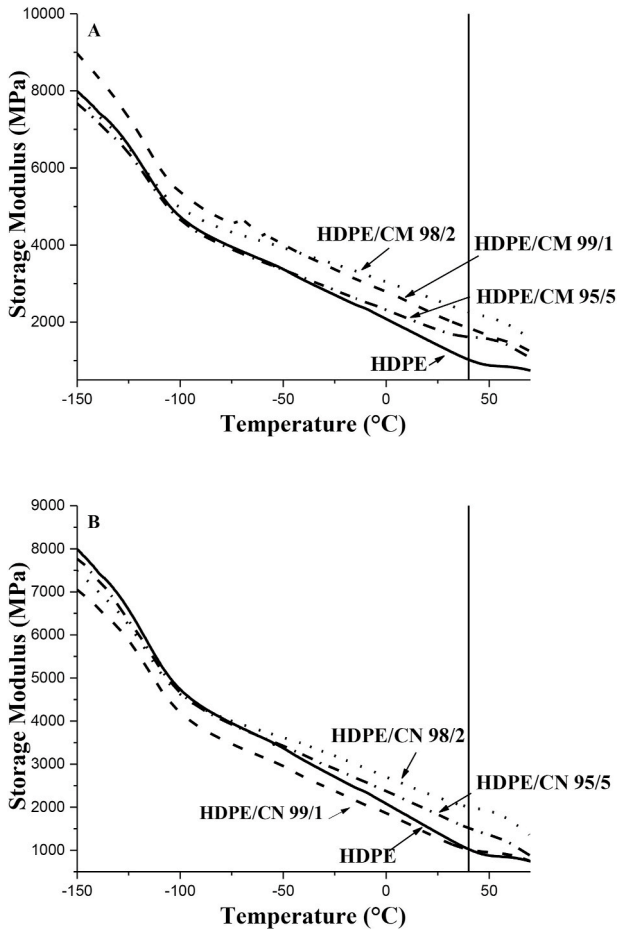

Fig. 4. A) Storage modulus (E′) of HDPE/CM and B) Storage modulus (E′) of HDPE/CN composites.

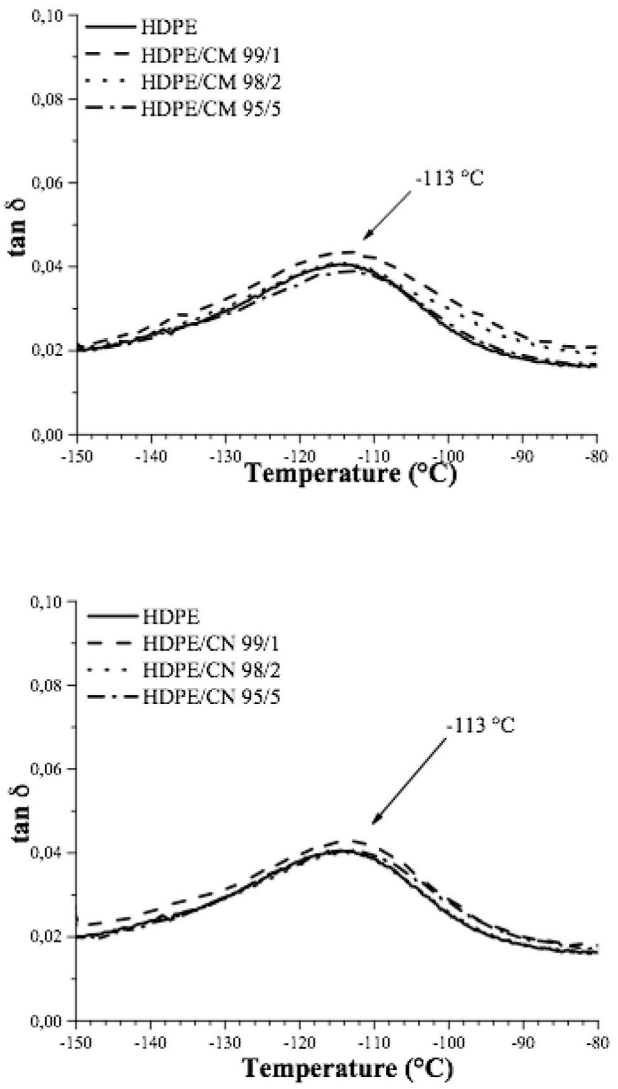

Fig. 5. A) Tanδ of HDPE/CM composites B) Tanδ of HDPE/CN composites.

Modified Eagle Medium) supplemented with 10% fetal bovine serum (Life Technologies, Milan, Italy), 100 U/ml penicillin, 100 μg/ml streptomycin, were passaged at subconfluency to prevent contact inhibition and were kept under a humidified atmosphere of 5% CO_2 in air, at 37 °C. Cell adhesion on grafts was evaluated using a 24-well plate at 10 min post seeding. Cells were detached using trypsin for 3 min, carefully counted and seeded at 2 x 10^3 cells/disk in 100 μl of growth medium on the samples. The 24-well plates were kept at 37 °C, 0.5% CO_2 for 15 min. The grafts were carefully washed with Phosphate Buffer Solution (PBS) and then stained with DAPI (4′,6-diamidino-2-phenylindole dihydrochloride) in order to stain the nuclei [33,34]. The number of adherent cells was determined by counting the number of DAPI-positive nuclei. Cells were plated at a density of 2500 cells/sample in 24-well and then transferred into the bioreactor. After 24 h, cell viability was assessed by Cell Titer GLO (Promega, Milan, Italy). Fibroblasts were seeded at a concentration of 5000 cells/sample in a 24-well plate and then transferred into the bioreactor. After 24 h, cells were fixed in 2.5% glutaraldehyde in Phosphate Buffer Saline (PBS) and then dehydrated using progressive incubation in ethanol. The cell morphology was observed by SEM.

3. Results and discussion

Table 1 reports characteristics of the two chitosan powders. The DD, obtained by FTIR, is 97 for CN and 87% for CM. The values correspond to those given in the technical sheet of the commercial products. WAXD patterns of CM and CN present two peaks at about 2θ = 10.4° (hkl 020) and 2θ = 20.1° (hkl 110) [35].

The crystalline indexes (Table 1) calculated by the area method (χ_C (%)) and peaks intensity (χ_{CI} (%)), even if different from each other due to the different method of evaluation, indicate that CM is more crystalline than CN (see Fig. 1). In general chitosan crystallinity decreases with DD [35], according to the findings of the present work. The TG thermograms in N_2 of CM and CN show two main decomposition steps (Fig. 2). The first decomposition appears in the range from 50 to 100 °C with a weight loss of about 7.9 and 8.9% for CM and CN, respectively.

Table 2
Young modulus (***E***), elongation at break (ε_b) and tensile strength at break (σ_b) by stress – strain experiments for HDPE/chitosan composites.

	(E) (MPa)	(σ_b) (MPa)	(ε_b) (%)		(E) (MPa)	(σ_b) (MPa)	(ε_b) (%)
HDPE	969 ± 17	13.7 ± 0.4	320 ± 52	HDPE	969 ± 17	13.7 ± 0.4	320 ± 52
HDPE/CM 99/1	1057 ± 49	14.8 ± 4.2	22 ± 6	HDPE/CN 99/1	1071 ± 54	15.2 ± 0.4	148 ± 53
HDPE/CM 98/2	1069 ± 45	15.2 ± 1.8	19 ± 4	HDPE/CN 98/2	1088 ± 36	15.0 ± 1.0	29 ± 11
HDPE/CM 95/5	1219 ± 74	19.7 ± 2.4	10 ± 2	HDPE/CN 95/5	1117 ± 34	15.7 ± 1.5	17 ± 2

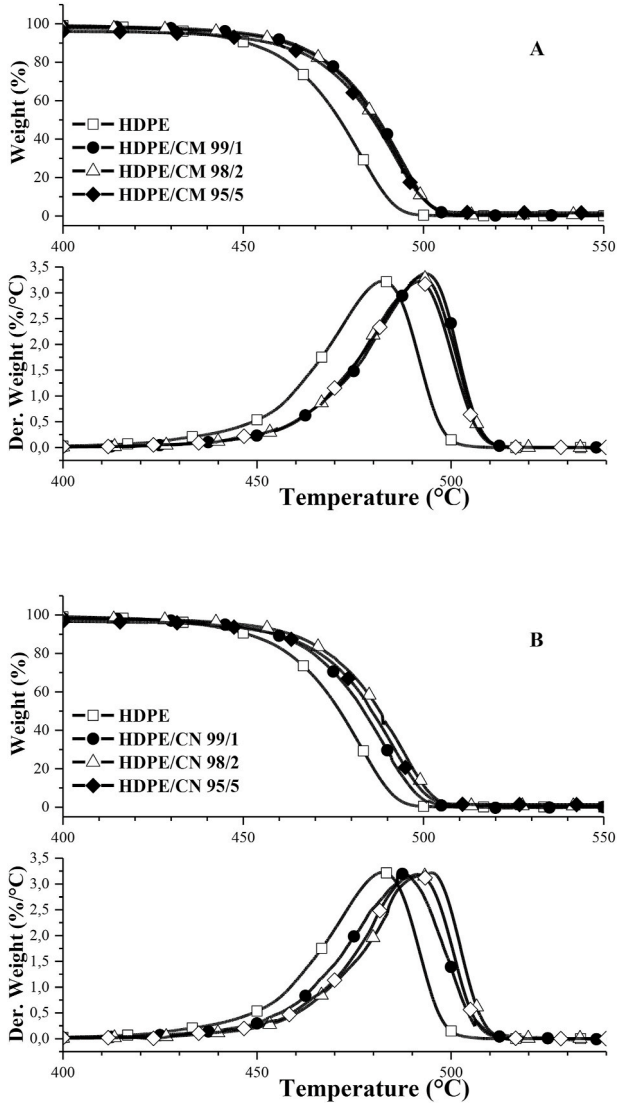

Fig. 6. A) TG and dTG curves of the HDPE/CM composites and B) the HDPE/CN composites.

Table 3
Thermogravimetric parameters of HDPE/Chitosan composites.

	CM loading (wt.%)					CN loading (wt.%)			
	Blank	1	2	5		Blank	1	2	5
T_{10}	451	463	462	458	T_{10}	451	459	463	459
T_{max}	477	493	492	492	T_{max}	477	488	492	491

The second step, due to the decomposition of the saccharide backbones, starts at 260 °C for both chitosan powders. In air, the first decomposition is similar to that in N_2, the second one occurs at 225 °C. Finally, the residues are further oxidized to CO and CO_2 in 330°C and 560 °C range. The results indicate that both chitosan powders are processable at HDPE processing temperature (i.e. 190 °C). Furthermore, T_{max} values for both CM and CN are similar (302°C vs. 296°C in N_2 and 270°C and 273 °C in air, respectively), hence indicating that the chitosan powders exhibit the same thermal stability.

The micrograph analysis of the composites cross-sections, presented in Fig. 3, indicates that the addition of chitosan to the HDPE matrix leads to an extended phase separation. No interaction seems to occur between the chitosan fillers and the polymer matrix. As a result, chitosan

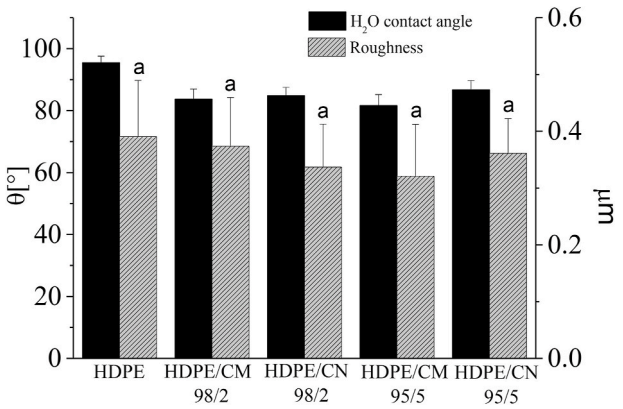

Fig. 7. Water contact angle values (black bars) and surface roughness (R_a) (gray bar) for HDPE and HDPE/chitosan composites. The letter *a* indicates no significant differences ($p > 0.05$) when analysed by Kruskal-Wallis test.

aggregates are visible on the section surface, and the size and number of the aggregates increases with the chitosan loading. These aggregates are bigger and elongated in HDPE/CM composites (≈100–200 μm), smaller and rounded in HDPE/CN ones (≈10–15 μm). The absence of voids in the matrix after fracture suggests that the interfacial shear strength between the filler and the matrix is not very weak [36].

In all the composites, HDPE crystallizes in the orthorhombic form [37] (not reported figures for sake of brevity), highlighting that the presence of chitosan does not influence the crystalline structure of the HDPE. Moreover, the crystallinity degree of HDPE in the composites is similar to that of neat polymer (i.e. 69 ± 2%), independently on the composition and the type of chitosan.

Fig. 4 shows the storage modulus (E′) as a function of the temperature for all the systems. From an overall point of view, the main effect exerted by the presence of both types of chitosan is the increase of the storage moduli E' in the rubbery plateau at 40 °C: this temperature is relevant considering the possible biomedical application of these materials.

The highest (E′) value is shown when 2 wt% chitosan is used. In particular, E' passes from about 1000 MPa for blank HDPE to about 2200 MPa for HDPE/CM 98/2 (120% increase as compared to unfilled polymer) and to 2000 MPa for HDPE/CN 98/2 (100% increase as compared to unfilled polymer).

In general, CM always shows a higher reinforcing effect with respect to CN, probably due to the higher crystallinity degree of CM with respect to CN counterpart.

Fig. 5 shows tanδ curves for all the systems in the range of −150°C to 80°C in order to highlight the γ transition of HDPE (that corresponds to the T_g and appears at about −113°C accordingly to literature [38]). The presence of CM and CN does not affect the T_g of HDPE. These results can be explained considering the different polarity of the composite components and the gross phase separation of chitosan in HDPE, as observed by SEM. They also exclude a possible partial miscibility between the two polymers.

Table 2 reports the Young modulus, stress and strain at break values for the HDPE/chitosan composites as a function of the filler content, compared to those of the neat HDPE. As expected, the pure polymer displays a ductile behavior with elongation and stress at break of roughly 320% and 14 MPa respectively. The addition of chitosan to the polymer matrix results in a sharp decrease in the elongation at break achieving 22 and 148% for 1 wt% CM and CN compounds, respectively. Interestingly, HDPE/CN 99/1 still displays a ductile behavior (stress strain curves not reported for sake of brevity). Further increasing of CM and CN loadings to 5 wt% decreases the elongation at break to 10 and 17%, respectively. These results are in general observed in non-compatible polymer blends [36]. The presence of chitosan can restrict

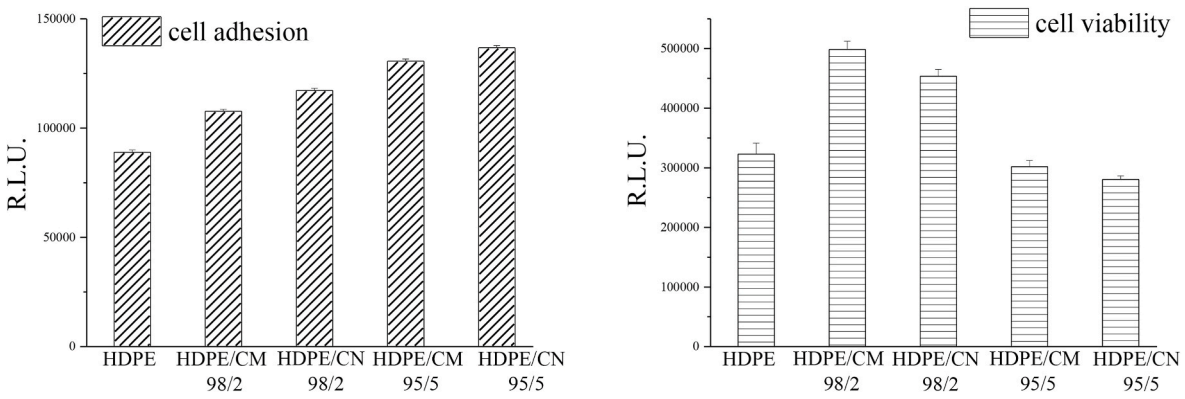

Fig. 8. Adherent fibroblast per field at 10 min (A) and the viable cells after 24 h (B) of HDPE/chitosan composites.

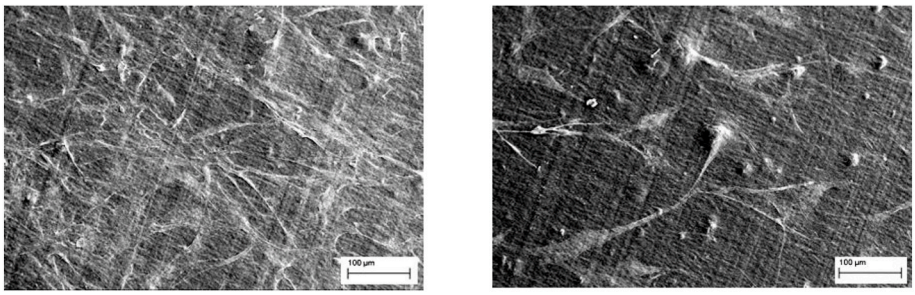

Fig. 9. Fibroblast morphology observed on HDPE/CN 98/2 (A) and HDPE/CN 95/5 (B).

the mobility of the polymer molecules to flow freely on each other causing premature failure. However, the stress at break increases from 13.7 for neat HDPE to 15.7 MPa for HDPE/CN 95/5 and 19.7 MPa for HDPE/CM 95/5, indicating that, despite the incompatibility, there is no complete lack of interfacial adhesion between the components of the composite structure [36]. This result is in agreement with morphological characterization by SEM. The elastic modulus *E* of the composites increases with the amount of chitosan (that is stiffer as compared to HDPE), irrespective of the type used.

Fig. 6 shows TG and dTG curves for HDPE composites recorded in N_2. T_{10} and T_{max}, (i.e. the temperatures corresponding to 10% weight loss and to the maximum of the derivative curves, respectively) are listed in Table 3. HDPE and all the chitosan-HDPE systems show a single degradation step; in addition, the thermal stability of the polymer matrix is enhanced by the presence of both type of chitosan. This effect is more evident for $T_{max,}$ which increases up to 16°C in presence of chitosan. However, the degradation process does not seem to be related to the amount and the type of chitosan powder. This finding can be explained as chitosan can act as a barrier for the diffusion of the degradation products of the polymer matrix [39,40,41].

Fig. 7 shows water contact angle and surface roughness values for HDPE and its composites. Neat HDPE shows a water contact angle of 95.5 ± 2.1°, in accordance with literature [42]. All the composites have a slightly lower contact angle value (about 10° lower than that of the neat polymer) with no significant differences as far as the chitosan loading is considered. The lowest contact angle value is found for HDPE/CM 95/5 (i.e. 81.6 ± 3.6). This increase in wettability is not dependent on the surface roughness. In fact, according to the Kruskal-Wallis test ($p > 0.05$), there are no significant differences between the surface microroughness of HDPE and its composites (Fig. 7). This result is in agreement with our previous outcomes that suggest that surface roughness is not the only parameter affecting wettability [43,44]. Indeed, in this case, the ruling parameter seems the polarity induced by the chitosan presence, that plays a fundamental role in increasing the wettability of HDPE composites.

Fig. 8 shows cell adhesion at 10 min (A) and cell viability after 24 h (B) of the HDPE and HDPE/chitosan composites. All the composites sustain a faster cell adhesion (Fig. 8A), compared to unfilled HDPE. In addition, by increasing the chitosan content, cell adhesion increases. This finding may result from the electrostatic interactions between the negative charges of the surface of cell membranes and the cationic sites on chitosan chains, as reported in literature [45–48]. Besides, cell adhesion seems also slightly influenced by the acetylation degree of the two chitosan powders. In particular, the charge density of CN is higher than that of CM, due to the lower acetylation degree of the former filler, making available a higher number of free amino groups exposed at the surface. This leads to greater cell adhesion in agreement with several scientific papers [49,50].

Conversely, cell viability pattern appears different from that of cell adhesion. In particular, the addition of 2 wt % of chitosan, irrespective of its DD, increases cell viability that in turn, decreases at higher chitosan loading (Fig. 8B). This behavior is consistent with the literature [50,51]. In fact, at 5 wt % loading, chitosan appears to exert a predominant cytostatic effect on fibroblasts [50], which may owe to the extremely high adhesion of fibroblasts on biomacromolecule, hindering cell proliferation [49].

Finally, it is worth underlining that, although a correlation between cell viability and roughness has been reported [42,43,51], in this work the main effect on cell interaction is given by the chemistry of chitosan (i.e. the availability of amino groups).

The results on cell viability are also consistent with the morphology of fibroblasts. As a qualitative assessment of cell morphology at 24 h, SEM micrographs of fibroblasts grown on the surface of HDPE CN 98/2 (Fig. 9A) and HDPE CN 95/5 (Fig. 9B) are shown. In Fig. 9A, cells are well interconnected and flat indicating that, after adhesion, a correct cellular spreading occurred and the material was capable to sustain cell viability. Conversely, a lower number of adherent fibroblasts can be seen in Fig. 9B, though, in both conditions, the same number of cells was initially plated: fibroblasts appear spindle-shaped and intermixed with some spherical cellular debris, likely belonging to apoptotic cells.

4. Conclusions

In this work, HDPE/chitosan composites have been prepared by melt extrusion technique with the purpose to obtain novel bio-composites suitable for biomedical applications, like subdermal cranio-facial scaffolds. Two chitosan powders differing for degree of acetylation and molecular weight were used in different amounts (i.e. 1, 2 and 5 wt%).

The composites showed improved mechanical properties with respect the unfilled HDPE. In particular, the storage modulus at 40 °C for the system containing 2 wt% of chitosan significantly increased with respect to that of HDPE. Similarly, an increase of both Young modulus and tensile strength was observed in tensile tests; conversely, both the fillers reduced the HDPE elongation at break.

Furthermore, cell adhesion increases with the increase of chitosan loadings. Conversely, the maximum of cell viability was observed for the composites containing 2 wt% of biomacromolecule. This finding is ascribed to the cytostatic effect of chitosan, which became predominant at 5 wt% loading.

Besides, the surface roughness and wettability were not involved in the biological behavior of the composites, which seems to depend only on the chemistry of chitosan.

Data availability

The raw/processed data required to reproduce these findings cannot be shared at this time as the data also forms part of an ongoing study.

CRediT Author Statement

Mattia Di Maro: samples preparation, thermal and mechanical characterization; Maria Giulia Faga: general conceptualization, microstructural analysis and supervision; Giulio Malucelli: conceptualization dealing with preparation methods and mechanical charaterization, Federico Mussano: concept, review and editing of biological data; Tullio Genova: biological data acquisition and analysis; Rania Morsi: conceptualization dealing with materials design and powder analysis; Amal Hamdy: funding acquisition and resources; Donatella Duraccio: general conceptualization, funding acquisition and supervision.

Declaration of competing interest

The authors declare that they have no known competing financial interests or personal relationships that could have appeared to influence the work reported in this paper.

Acknowledgements

The authors acknowledge the support from the “Ministero Italiano degli Affari Esteri e della Cooperazione Internazionale-MAECI”, Joint project n. PGR000701 (2016/2018) and from the Egyptian Science & Technology Development Fund (STDF), Italy-Egypt joint cooperation project no. 25997. The authors also thanks Prof. Finizia Auriemma from the University of Naples (UNINA) and Dr. Marcella Bidoccu from the IMAMOTER-CNR for fruitful discussion on DMTA and statistical analysis, respectively.

Appendix A. Supplementary data

Supplementary data to this article can be found online at https://doi.org/10.1016/j.polymertesting.2020.106610.

References

[1] D. Puppi, F. Chiellini, A.M. Piras, E. Chiellini, Polymeric materials for bone and cartilage repair, Prog. Polym. Sci. 35 (2010) 403–440, https://doi.org/10.1016/j.progpolymsci.2010.01.006.

[2] N.C. Paxton, M.C. Allenby, P.M. Lewis, M.A. Woodruff, Biomedical applications of polyethylene, Eur. Polym. J. 118 (2019) 412–428, https://doi.org/10.1016/j.eurpolymj.2019.05.037.

[3] M. Wang, Developing bioactive composite materials for tissue replacement, Biomater 24 (2003) 2133–2215, https://doi.org/10.1016/S0142-9612(03)00037-1.

[4] M.T. Lam, J.C. Wu, Biomaterial applications in cardiovascular tissue repair and regeneration, Expert Rev. Cardiovasc Ther. 10 (2012) 1039–1049, https://doi.org/10.1586/erc.12.99.

[5] F. Bronner, M. Farach-Carson, A. Mikos, Engineering of Functional Skeletal Tissues, Springer London, London, 2007.

[6] S.P. Lake, S. Ray, A.M. Zihni, D.M. Thompson, J. Gluckstein, C.R. Deeken, Pore size and pore shape – but not mesh density – alter the mechanical strength of tissue ingrowth and host tissue response to synthetic mesh materials in a porcine model of ventral hernia repair, J. Mech. Behav. Biomed. Mat. 42 (2015) 186–197, https://doi.org/10.1016/j.jmbbm.2014.11.011.

[7] V. Karageorgiou, D. Kaplan, Porosity of 3D biomaterial scaffolds and osteogenesis, Biomat 26 (2005) 5474–5491, https://doi.org/10.1016/j.biomaterials.2005.02.002.

[8] J.R.M. James, P. Wingo, Implants for Cranioplasty, 1994. US5545226 A.

[9] P.A.D. Rubin, Orbital Implant, 1993. US5466258 A.

[10] W. Bonfield, M.D. Grynpas, A.E. Tully, J. Bowman, J. Abram, Hydroxyapatite reinforced polyethylene - a mechanically compatible implant material for bone replacement, Biomat 2 (1981) 185–186, https://doi.org/10.1016/0142-9612(81)90050-8.

[11] R.E. Swain, M. Wang, B. Beale, W. Bonfield, HAPEX (TM) for otologic applications, Biomed. Eng. Appl. Basis Commun. 11 (1999) 315–320.

[12] S. Mira, T. Yasin, P.J. Halley, H.M. Siddiqi, T. Nicholson, Thermal, rheological, mechanical and morphological behavior of HDPE/chitosan composite, Carbohydr. Polym. 83 (2011) 414–442, https://doi.org/10.1016/j.carbpol.2010.07.069.

[13] P.T. Ton That, K.E. Tanner, W. Bonfield, Fatigue characterization of a hydroxyapatitereinforced polyethylene composite. I. Uniaxial fatigue, J. Biomed. Mater. Res. 51 (2000) 453–460, https://doi.org/10.1002/1097-4636.

[14] A. Yari Sadi, S.S. Homaeigohar, A.R. Khavandi, J. Javadpour, The effect of partially stabilized zirconia on the mechanical properties of the hydroxyapatite–polyethylene composites, J. Mater. Sci. Mater. Med. 15 (2004) 853–858, https://doi.org/10.1023/B:JMSM.0000036272.28022.3a.

[15] M. Wang, L.L. Hench, W. Bonfield, Bioglass®/high density polyethylene composite for soft tissue applications: preparation and evaluation, J. Biomed. Mater. Res. 42 (1998) 577–586, https://doi.org/10.1002/(SICI)1097-4636(19981215)42:4<577:AID-JBM14>3.0.CO;2-2.

[16] J. Huang, L. Di Silvio, M. Wang, I. Rehman, C. Ohtsuki, W. Bonfield, Evaluation of in vitro bioactivity and biocompatibility of Bioglass®-reinforced polyethylene composite, J. Mat. Sci.: Mat in Med. 8 (1997) 809–813, https://doi.org/10.1023/A:1018581100400.

[17] P. Lima, R. Brito, B. Santos, A. Tavares, P. Agrawal, D. Andrade, S. Silva, Rheological properties of HDPE/chitosan composites modified with PE-g-MA, J. Mat. Res. 32 (2017) 775–787, https://doi.org/10.1557/jmr.2016.519.

[18] M.J.G. De Araújo, R.C. Barbosa, M.V.L. Fook, E.L. Canedo, S.M.L. Silva, E. S. Medeiros, I.F. Leite, HDPE/Chitosan blends modified with organobentonite synthesized with quaternary ammonium salt impregnated chitosan, Mat 11 (2018) 291–305, https://doi.org/10.3390/ma11020291.

[19] C. Vasile, R.N.D. Catalina, N. Cheaburu, Y.G.M. Pricope, M. Bračič, D. Pamfila, G. E. Hitruc, D. Duraccio, Low density polyethylene – chitosan composites, Comp Part B: Eng. 55 (2013) 314–323, https://doi.org/10.1016/j.compositesb.2013.06.008.

[20] M. Dash, F. Chiellini, R.M. Ottenbrite, E. Chiellini, Chitosan—a versatile semi-synthetic polymer in biomedical Applications, Prog. Polym. Sci. 36 (2011) 981–1014, https://doi.org/10.1016/j.progpolymsci.2011.02.001.

[21] M.N. Kumar, R.A. Muzzarelli, C. Muzzarelli, H. Sashiwa, A.J. Domb, Chitosan chemistry and pharmaceutical perspectives, Chem. Rev. 104 (2004) 6017–6084, https://doi.org/10.1021/cr030441b.

[22] R.A.A. Muzzarelli, Natural Chelating Polymers; Alginic Acid, Chitin, and Chitosan, Pergamon Press Oxford, New York, 1973, 254 pp.

[23] R. Jayakumar, N. Nwe, S. Tokura, H. Tamura, Sulfated chitin and Chitosan as novel biomaterials, Int. J. Biol. Macromol. 40 (2007) 175–181, https://doi.org/10.1016/j.ijbiomac.2006.06.021.

[24] M. Rinaudo, Main properties and current applications of some polysaccharides as biomaterials, Polym. Int. 57 (2008) 397–430, https://doi.org/10.1002/pi.2378.

[25] V.K. Mourya, N.N. Inamdar, Chitosan-modifications and applications: opportunities galore, React. Funct. Polym. 68 (2008) 1013–1051, https://doi.org/10.1016/j.reactfunctpolym.2008.03.002.

[26] K. Kurita, Chitin and chitosan: functional biopolymers from marine crustaceans, Mar. Biotechnol. 8 (2006) 203–226, https://doi.org/10.1007/s10126-005-0097-5.

[27] H. Mittala, S. Sinha Ray, B.S. Kaith, J.K. Bhatia, Sukriti, J. Sharma, S.M. Alhassan, Recent progress in the structural modification of Chitosan for applications in diversified biomedical fields, Eur. Polym. J. 109 (2018) 402–434, https://doi.org/10.1016/j.eurpolymj.2018.10.013.

[28] R. Sedghi, M. Gholami, A. Shaabani, M. Saber, H. Niknejad, Preparation of novel chitosan derivative nanofibers for prevention of breast cancer recurrence, Eur. Polym. J. 12315 (2020), https://doi.org/10.1016/j.eurpolymj.2019.109421. Article 109421.

[29] R.J. de Groot, J.M. Rieger, A.J.W.P. Rosenberg, M.A.W. Merkx, C.M. Speksnijder, A pilot study of masticatory function after maxillectomy comparing rehabilitation with an obturator prosthesis and reconstruction with a digitally planned, prefabricated, free, vascularized fibula flap, J. Prosthet. Dent (2020 Jan 17), https://doi.org/10.1016/j.prosdent.2019.06.005.

[30] K.V. Reesha, S.K. Panda, J. Bindu, T.O. Varghese, Development and characterization of an LDPE/chitosan composite antimicrobial film for chilled fish storage, Int. J. Biol. Macromol. 79 (2015) 934–942, https://doi.org/10.1016/j.ijbiomac.2015.06.016.
[31] A. Baxter, M. Dillon, K.D.A. Taylor, G.A.F. Roberts, Improved method for IR determination of the degree of N-acetylation of Chitosan, Int. J. Biol. Macromol. 14 (1992) 166–169, https://doi.org/10.1016/S0141-8130(05)80007-8.
[32] B. Focher, P.L. Beltrame, A. Naggi, G. Torri, Alkaline N-deacetylation of chitin enhanced by flash treatments. Reaction kinetics and structure modifications, Carbohydr. Polym. 12 (1990) 405–418, https://doi.org/10.1016/0144-8617(90)90090-F.
[33] T. Genova, G.P. Grolez, C. Camillo, M. Bernardini, A. Bokhobza, E. Richard, M. Scianna, L. Lemonnier, D. Valdembri, L. Munaron, M.R. Philips, V. Mattot, G. Serini, N. Prevarskaya, D. Gkika, A. Fiorio Pla, TRPM8 inhibits endothelial cell migration via a non-channel function by trapping the small GTPase, Rap. J. Cell Biol. 216 (2017) 2107–2130, https://doi.org/10.1083/jcb.201506024.
[34] F. Mussano, T. Genova, P. Rivolo, P. Mandracci, L. Munaron, M.G. Faga, S. Carossa, Role of surface finishing on the in vitro biological properties of a silicon nitride–titanium nitride (Si_3N_4–TiN) composite, J. Mat. Sci. 52 (2017) 467–477, https://doi.org/10.1007/s10853-016-0346-1.
[35] M. Jaworska, K. Sakurai, P. Gaudon, E. Guibal, Influence of chitosan characteristics on polymer properties. I: crystallographic properties, Polym. Int. 52 (2003) 198–205, https://doi.org/10.1002/pi.1159.
[36] A. Benhamida, M. Kaci, S. Cimmino, C. Silvestre, D. Duraccio, Evaluation of the effectiveness of new compatibilizers based on EBAGMA-LDPE and EBAGMA-PET masterbatches for LDPE/PET composites, Macromol. Mater. Eng. 295 (2010) 222–232, https://doi.org/10.1002/mame.200900290.
[37] C.W. Bunn, The crystal structure of long-chain normal paraffin hydrocarbons. The “shape” of the CH2 group, Trans. Faraday Soc. 35 (1939) 482–491.
[38] F.C. Stehling, L. Mandelkern, The glass temperature of linear polyethylene, Macromolecules 3 (1970) 242–252.
[39] B. Singh, N. Sharma, Mechanistic implications of plastic degradation, Polym. Degrad. Stabil. 93 (2008) 561–584, https://doi.org/10.1016/j.polymdegradstab.2007.11.008.
[40] K. Chrissafis, K.M. Paraskevopoulos, E. Pavlidou, D. Bikiaris, Thermal degradation mechanism of HDPE nanocomposites containing fumed silica nanoparticles, Thermochim. Acta 485 (2009) 65–71, https://doi.org/10.1016/j.tca.2008.12.011.
[41] S. Sinha Ray, M. Bousmina, Biodegradable polymers and their layered silicate nanocomposites: in greening the 21st century materials world, Prog. Mater. Sci. 50 (2005) 962–1079, https://doi.org/10.1016/j.pmatsci.2005.05.002.
[42] S.L. Favaro, A.F. Rubira, E.C. Muniz, E. Radovanovic, Surface modification of HDPE, PP, and PET films with KMnO4/HCl solutions, Polym. Degrad. Stabil. 92 (2007) 1219–1226, https://doi.org/10.1016/j.polymdegradstab.2007.04.005.
[43] D. Duraccio, V. Strongone, G. Malucelli, F. Auriemma, C. De Rosa, F.D. Mussano, T. Genova, M.G. Faga, The role of alumina-zirconia loading on the mechanical and biological properties of UHMWPE for biomedical applications, Comp. Part B 164 (2019) 800–808, https://doi.org/10.1016/j.compositesb.2019.01.097.
[44] D. Duraccio, V. Strongone, M.G. Faga, F. Auriemma, F.D. Mussano, T. Genova, G. Malucelli, The role of different dry-mixing techniques on the mechanical and biological behavior of UHMWPE/alumina-zirconia composites for biomedical applications, Eur. Polym. J. 120 (2019) 109274, https://doi.org/10.1016/j.eurpolymj.2019.109274.
[45] C. Hadjicharalambous, C. Flouraki, R. Narain, M. Chatzinikolaidou, M. Vamvakaki, Controlling pre-osteoblastic cell adhesion and spreading on glycopolymer brushes of variable film thickness, J. Mater. Sci. Mater. Med. 26 (2018) 98–108, https://doi.org/10.1007/s10856-018-6112-y.
[46] J.K.F. Suh, H.W.T. Matthew, Application of chitosan-based polysaccharide biomaterials in cartilage tissue engineering: a review, Biomaterials 21 (2000) 2589–2598.
[47] W.Y. Chuang, T.H. Young, C.H. Yao, W.Y. Chiu, Properties of the poly(vinyl alcohol)/chitosan composite and its effect on the culture of fibroblast in vitro, Biomater 20 (1999) 1479–1487, https://doi.org/10.1016/S0142-9612(00)00126-5.
[48] T. Koyano, N. Minoura, M. Nagura, K. Kobayashi, Attachment and growth of cultured fibroblast cells on PVA/chitosan-compositeed hydrogels, J. Biomed. Mater. Res. 39 (1998) 486–490, https://doi.org/10.1002/(SICI)1097-4636(19980305)39:3<486:AID-JBM20>3.0.CO;2-7.
[49] T. Freier, H.S. Koh, K. Kazazian, M.S. Shoichet, Controlling cell adhesion and degradation of chitosan films by N-acetylation, Biomater 29 (2005) 5872–5878, https://doi.org/10.1016/j.biomaterials.2005.02.033.
[50] C. Chatelet, O. Damour, A. Domard, Influence of the degree of acetylation on some biological properties of chitosan films, Biomater 22 (2001) 261–268, https://doi.org/10.1016/S0142-9612(00)00183-6.
[51] M. Izume, T. Taira, T. Kimura, T. Miyata, A novel cell culture matrix composed of chitosan and collagen complex, in: G. Skjak-Braëk, T. Anthonsen, P. Sandford (Eds.), Chitin and Chitosan, Elsevier Applied science, Amsterdam, 1989, pp. 653–666.